

Protein S-Glutathiolation Triggered by Decomposed S-Nitrosoglutathione[†]

Limei Tao and Ann M. English*

Department of Chemistry and Biochemistry, Concordia University, 7141 Sherbrooke Street West, Montreal, Quebec, Canada H4B 1R6

Received October 28, 2003; Revised Manuscript Received February 2, 2004

ABSTRACT: Recombinant human brain calbindin D_{28K} (rHcBP), human Cu,Zn-superoxide dismutase (HCuZnSOD), rabbit muscle glyceraldehyde-3-phosphate dehydrogenase (GAPDH), and bovine serum albumin (BSA) were found to be S-glutathiolated in decomposed S-nitrosoglutathione (GSNO) solutions. Tryptic or Glu-C digestion and MALDI-TOF MS analyses of the digests are consistent with S-thiolation of Cys111 and Cys187 of HCuZnSOD and rHcBP, respectively, upon exposure to decomposed GSNO. GAPDH activity analysis reveals that S-glutathiolation most likely occurs on the active site Cys149, and the single free Cys34 is assumed to be the site of S-glutathiolation in BSA. The yields of S-glutathiolation of rHcBP, GAPDH, and BSA were much higher than those of HCuZnSOD. The latter is limited by the accessibility of Cys111 to the glutathiolating reagent in the HCuZnSOD dimer. Unlike decomposed GSNO, fresh GSNO, reduced glutathione (GSH), and oxidized glutathione (GSSG) are not efficient S-glutathiolating agents for the proteins examined here. On the basis of analysis by mass spectrometry and UV–visible absorption, GSNO decomposition in the dark at room temperature yields glutathione disulfide S-oxide [GS(O)SG], glutathione disulfide S-dioxide (GSO₂SG), and GSSG as products. GS(O)SG is the efficient protein S-glutathiolating agent in GSNO solutions, not GSNO, which does not carry out efficient S-glutathiolation of rHcBP, HCuZnSOD, or GAPDH *in vitro*. A hydrolysis pathway yielding GSOH and nitroxyl (HNO/NO[−]) as intermediates is proposed for GSNO decomposition in the dark. This is based on inhibition of GSNO breakdown by dimedone, a reagent specific for sulfenic acids, and on nitroxyl scavenging by metmyoglobin. The results presented here are contrary to numerous reports of protein S-thiolation by low-molecular weight S-nitrosothiols.

Protein S-thiolation is a reversible oxidative modification that involves disulfide linkage of GSH¹ (S-glutathiolation), or related low-molecular weight thiols such as cysteine, to proteins *in vivo* (1, 2). Protein S-glutathiolation was introduced into the field of redox biochemistry almost 50 years ago as a possible mechanism of protein regulation in response to changes in the intracellular redox status (3). Currently, protein S-glutathiolation is being reinvestigated as a mechanism of redox- and NO-mediated signal transduction as well

as a cellular response to oxidative and/or nitrosative stress (4, 5). Interrelations between S-glutathiolation, thiol oxidation, and S-nitrosation leading to the formation of mixed disulfides between protein thiols and the tripeptide GSH may serve to transduce oxidative and nitrosative stimuli into a functional response at various levels of cellular signaling (3).

Stress-induced protein S-thiolation is poorly understood. Several mechanisms have been proposed for protein S-glutathiolation, including (a) thiol–disulfide exchange between a protein thiol and GSSG (6), (b) oxidation of a protein thiol by oxy radicals or H₂O₂ to form a thiyl radical or sulfenic acid that reacts with GSH to produce a mixed disulfide (7), (c) oxidation of GSH to the sulfenic acid GSOH that reacts with a protein thiol to form a mixed disulfide (8), (d) nucleophilic attack of a protein thiolate on GSNO to produce a mixed disulfide (5, 8–10), and (e) S-nitrosation of a protein thiol followed by reaction with GSH to yield a mixed disulfide (5, 8).

Numerous groups have reported protein S-thiolation by low-molecular weight S-nitrosothiols (RSNO) (5, 8–12). The list includes many proteins that contain activated cysteine residues such as aldose reductase (11), cathepsin K (9), glyceraldehyde-3-phosphate dehydrogenase (GAPDH) (10), papain (13), and caspase-3 (12). It has also been proposed (14) that a product of GSNO decomposition, GS(O)SG, is a protein glutathiolating agent. In this study, we compare protein S-glutathiolation in fresh and aged GSNO solutions. We recently reported that recombinant human brain calbindin

[†] This research was supported by a grant from the Canadian Institutes of Health Research to A.M.E. and a Garnet Strong Scholarship and Power Corporation/Desmarais and Archambault Graduate Fellowships to L.T.

* To whom correspondence should be addressed: Department of Chemistry and Biochemistry, Concordia University, 7141 Sherbrooke St. W., Montreal, Quebec, Canada H4B 1R6. E-mail: english@vax2.concordia.ca. Telephone: (514) 848-2424, ext 3338. Fax: (514) 848-2868.

¹ Abbreviations: ACTH, adrenocorticotrophic hormone; BSA, bovine serum albumin; dimedone, 5,5-dimethyl-1,3-cyclohexanedione; DTNB, 5,5'-dithiobis(2-nitrobenzoic acid); DTT, dithiothreitol; DTPA, diethylenetriamine-*N,N,N',N',N''*-pentaacetic acid; ESI-MS, electrospray ionization mass spectrometry; GAPDH, glyceraldehyde-3-phosphate dehydrogenase; GSH, reduced glutathione; GSNO, S-nitrosoglutathione; GSOH, glutathionesulfenic acid; GS(O)SG, glutathione disulfide S-oxide or glutathione thiosulfinate; GSO₂SG, glutathione disulfide S-dioxide or glutathione thiosulfonate; GSSG, oxidized glutathione; HCuZnSOD, human Cu,Zn-superoxide dismutase; MALDI, matrix-assisted laser desorption ionization; NEM, *N*-ethylmaleimide; neocuproine, 2,9-dimethyl-1,10-phenanthroline; QTOF, quadrupole time-of-flight; rHcBP, recombinant human brain calbindin D_{28K}; RSNO, low-molecular weight S-nitrosothiol; TNB^{2−}, 5-thio-2-nitrobenzoate anion.

D_{28K} (rHcCaBP), a Ca²⁺-binding protein noted for its abundance and specific distribution in mammalian brain and sensory neurons, has five free thiols and is readily S-glutathiolated *in vitro* (15). Since rHcCaBP has not been reported to be S-glutathiolated *in vivo*, modifications of human Cu,Zn-superoxide dismutase (HCuZnSOD), GAPDH, and BSA triggered by GSNO were also investigated. S-Thiolated forms of HCuZnSOD have been isolated from normal cells and from cells of individuals with amyotrophic lateral sclerosis (16–18). GAPDH has been identified as a major S-glutathiolated protein in endothelial cells and in rat heart under oxidative stress (19, 20), and was reported to be S-glutathiolated by GSNO *in vitro* as well as in endothelial cells (10). Serum albumin is the most abundant protein in plasma and is assumed to play an antioxidant role because of its scavenging of reactive oxygen and nitrogen species (21–23). The group responsible for this property of BSA is its only free thiol on Cys34, which comprises ~80% of the total free thiols in plasma (21).

A mechanism for rHcCaBP, HCuZnSOD, GAPDH, and BSA S-glutathiolation triggered by GSNO breakdown is proposed here. GSNO is hydrolyzed to glutathionesulfenic acid (GSOH) and nitroxyl (HNO/NO⁻). The reaction of GSOH with GSNO or dimerization of GSOH yields glutathione disulfide *S*-oxide [GS(O)SG], which is the active protein S-glutathiolating agent (14) in GSNO solutions. The results obtained upon addition of sulfenic acid and nitroxyl scavengers support the proposed mechanism.

MATERIALS AND METHODS

Materials. Recombinant His-tagged human brain calbindin D_{28K} (rHcCaBP) was prepared as described previously (15). The Ni-agarose-purified protein was dialyzed against 20 mM Tris-HCl (pH 7.4) containing 100 mM NaCl and 2 mM CaCl₂, and then digested with 1:100 (w/w) Factor Xa (Promega) for 18 h at room temperature to cleave the His tag. Any remaining His-tagged rHcCaBP was removed by rebinding the sample to the Ni-agarose beads. *S*-Nitroso-glutathione (GSNO) was obtained from Cayman, diethylenetriaminepentaacetic acid (DTPA) from ICN Pharmaceuticals, 2,9-dimethyl-1,10-phenanthroline (neocuproine) from Fluka, and 5,5-dimethyl-1,3-cyclohexanedione (dimedone) from Aldrich. Glutathione (GSH), glutathione disulfide (GSSG), human Cu,Zn-superoxide dismutase (HCuZnSOD), catalase, horse heart myoglobin, bovine serum albumin (BSA), DL-dithiothreitol (DTT), human [Glu¹]fibrinopeptide B, α -cyano-4-hydroxycinnamic acid, adrenocorticotrophic hormone (ACTH, fragment 1–10), rennin, and angiotensin I were from Sigma. Trypsin (modified sequencing-grade), bovine CuZnSOD, and rabbit muscle GAPDH were from Roche. 2-Propanol was from Fisher Scientific. Nanopure water (MilliQ) from a Millipore system was used to prepare all solutions.

Preparations of HCuZnSOD Stock Solutions. Commercial HCuZnSOD was reduced by incubating a 1 mg/mL solution with 5 mM DTT in 50 mM phosphate buffer (pH 7.4) at 30 °C for 1.5 h. The small reagents were removed on a NAP-5 1.3 cm \times 2.6 cm G25 column (Amersham Pharmacia Biotech) pre-equilibrated with N₂-saturated 50 mM Tris-HCl buffer (pH 7.4) or 50 mM ammonium acetate buffer (pH 4.0) for 1 h just before being used. Reduced HCuZnSOD was concentrated by ultrafiltration using an Ultrafree-0.5

centrifugal filter (Millipore) and incubated immediately after preparation with fresh or decomposed GSNO. The number of free cysteine residues was determined by monitoring on a Cary Varian spectrophotometer the absorbance at 412 nm ($\epsilon = 14.15 \text{ mM}^{-1} \text{ cm}^{-1}$) of the 5-thio-2-nitrobenzoate dianion (TNB²⁻) generated by the reaction of 200 μM DTNB with the free SH groups of 40 μM HCuZnSOD (24) in 100 mM potassium phosphate buffer (pH 7.27) containing 1 mM EDTA.

Preparation of GAPDH Stock Solutions. An ammonium sulfate suspension of GAPDH was diluted 2-fold with water and dialyzed (6000–8000 Da cutoff dialysis tubing) against water for 3 h, followed by three changes of 50 mM Tris-HCl buffer (pH 7.4) over a total of 48 h. The concentration of the resulting protein solution was determined spectrophotometrically ($\epsilon_{280} = 149 \text{ mM}^{-1} \text{ cm}^{-1}$) (25).

Preparation of BSA Stock Solutions. The number of free cysteine residues in BSA was determined as described above for HCuZnSOD. BSA was incubated with 2 mM DTT for 3 h at room temperature, and excess DTT was removed by dialysis (12000–14000 Da cutoff dialysis tubing) against 100 μM DTPA for 48 h with three changes. This procedure increased the number of free cysteines from 0.33 to 0.86 per BSA molecule.

Fresh and Decomposed GSNO Stock Solutions. Fresh GSNO solutions were prepared in MilliQ water just before being used and kept on ice. The GSNO concentration was determined spectrophotometrically [$\epsilon_{330} = 767 \text{ M}^{-1} \text{ cm}^{-1}$ (26)]. Decomposed GSNO was prepared by storing aqueous solutions at room temperature in the dark until no SNO absorption (334 nm) was detected (~60 h). Note that the GSNO solutions were always protected from light.

Nitroxyl Scavenging. Metmyoglobin was prepared (27) by oxidizing myoglobin with a 5% molar excess of potassium ferricyanide in 100 mM potassium phosphate buffer (pH 7.0). The low-molecular weight products were removed on a NAP-10 column equilibrated with MilliQ water, and metmyoglobin at a final concentration of 185 μM was incubated with 5 mM GSNO with and without 5 mM dimedone in water under anaerobic conditions at 20 °C in the dark. The reaction solutions were diluted 10-fold into degassed 100 mM potassium phosphate (pH 7.0) in a sealed 0.4 cm cuvette, and the spectrum of myoglobin was recorded. To measure the amount of GSNO remaining, myoglobin was removed by ultrafiltration using Ultrafree-0.5 centrifugal filters, and the absorbance at 330 nm was recorded in a 1 cm cuvette.

Reactivity of Proteins with GSNO, GSH, or GSSG. rHcCaBP was incubated with different molar ratios of GSNO, GSH, or GSSG in 50 mM Tris-HCl buffer (pH 7.4) for 20 min at 37 °C or room temperature. HCuZnSOD, GAPDH, and BSA were incubated in GSNO solutions under the conditions given in the figure legends.

UV-Vis Spectrophotometric Analyses. UV-vis measurements were used to investigate the decomposition of GSNO in the presence and absence of metal chelators or dimedone. Spectra were recorded in 1 cm cuvettes at 25 °C on a Beckman DU 650 spectrophotometer. Appropriate blanks, run under the same conditions, were subtracted from the sample spectra.

Mass Spectrometry. Electrospray ionization mass spectrometry (ESI-MS) was carried out on a Waters Micromass QTOF2 mass spectrometer. Protein samples (except BSA)

were exchanged into water on NAP-5 columns, concentrated by ultrafiltration using Ultrafree-0.5 centrifugal filters, and added to 60 μ L of a 50% acetonitrile/0.2% formic acid mixture to give final protein concentrations of 1–2 μ M. BSA was purified by dialysis against MilliQ water for 48 h with three changes, and diluted \sim 15-fold into a 20% methanol/5% acetic acid mixture to a final concentration of 5–10 μ M. Samples were directly infused into the Z-spray source of the QTOF2 apparatus at a flow rate of 1 μ L/min. Mass calibration was carried out using human [Glu¹]fibrinopeptide B. Protein mass spectra were deconvoluted using MaxEnt 1 software (Waters Micromass).

Peptide Mass Mapping. HCuZnSOD (\sim 20 μ g) was dissolved in a 60% acetonitrile/0.1% TFA mixture and dried on a Speed Vac. This step improved the digestion efficiency probably because HCuZnSOD is irreversibly unfolded to some extent in a 60% acetonitrile/0.1% TFA mixture, making the digestion sites more accessible. The sample was resuspended in 20 μ L of 100 mM Tris-HCl (pH 8.8) and heated to \sim 90 $^{\circ}$ C for 5 min to further denature the protein (28). After the sample had cooled in an ice/water bath, 2 μ L of trypsin (0.5 μ g/ μ L in 1% acetic acid) was added, the solution was incubated at 37 $^{\circ}$ C for 18 h, and digestion was stopped by freezing at -80° C. Peptides were desalted using C18 tips (ZipTip_{C18}, Millipore) and eluted from the tips with a 60% acetonitrile/0.1% TFA mixture. The eluate (1.5 μ L) was mixed with 1.5 μ L of matrix solution [100 μ L of α -cyano-4-hydroxycinnamic acid (40 mg/mL in acetone), 10 μ L of nitrocellulose (20 mg/mL in acetone), 40 μ L of acetone, and 50 μ L of 2-propanol], and 1.5 μ L of the peptide/matrix mixture was spotted onto a 96-well MALDI plate and air-dried. Samples were analyzed using a Waters Micromass M@LDI Analyzer mass spectrometer equipped with an N₂ laser (335 nm) and a time-of-flight (TOF) mass analyzer. The spectrometer was mass calibrated externally using ACTH, rennin, and angiotensin I.

RESULTS

S-Glutathiolation of rHCaBP. We have shown previously that Cys187 is readily S-thiolated but not the four other cysteine residues in His-tagged rHCaBP (15). After addition of GSNO to His-tagged rHCaBP, S-glutathiolation occurred rapidly and was independent of the incubation time over the interval from 5 to 180 min with GSNO (15). The His tag was cleaved from rHCaBP used in this study since we have evidence that this N-terminal modification alters the dimerization state and accessibility of the thiols in the protein (L. Tao, unpublished observations). It was reported that decomposed GSNO is a more effective S-glutathiolation reagent and less effective S-nitrosation reagent than fresh GSNO of glycogen phosphorylase *b* (8). To establish if this is the case with other proteins, a 5 mM solution of GSNO was left standing at room temperature in the dark until the SNO absorption at 334 nm was close to the baseline (Figure 1A, inset). Nontagged rHCaBP was incubated with the decomposed GSNO for 20 min, and although a negligible amount of GSNO remained in solution, rHCaBP was S-glutathiolated (+GS) to a much greater extent in decomposed than in fresh GSNO solutions (panel B vs panel A). On the other hand, S-nitrosation (+NO) is detected only in the presence of fresh GSNO (Figure 1A).

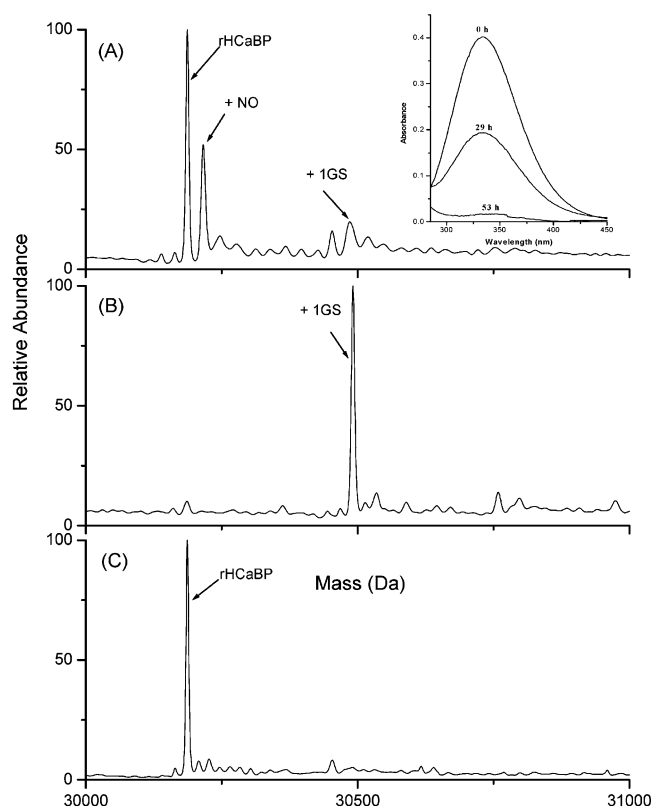


FIGURE 1: Effects of GSNO and GSSG on the S-glutathiolation of rHCaBP. rHCaBP was incubated with a 100-fold molar excess of (A) fresh GSNO or (B) decomposed GSNO and (C) a 50-fold excess GSSG for 20 min at 37 $^{\circ}$ C in 50 mM Tris-HCl buffer (pH 7.4). Samples for MS analysis were exchanged into water on a NAP-5 column, concentrated by ultrafiltration, and added to 60 μ L of a 50% acetonitrile/0.2% formic acid mixture to give a final protein concentration of 1–2 μ M. Samples were directly infused into the Z-spray source of the QTOF2 mass spectrometer at a flow rate of 1 μ L/min. The instrumental parameters were as follows: capillary voltage of 3.8 kV, cone voltage of 45 V, multiplier voltage of 550 V, MCP of 2100 V, and TOF of -9.1 kV. The inset shows UV-vis absorption of fresh and aged GSNO solutions. GSNO (5 mM) in water was allowed to stand at room temperature in the dark for 3 days. Aliquots were diluted 10-fold with water, and the spectra recorded in a 1 cm cuvette at 25 $^{\circ}$ C after 0, 29, and 53 h are shown.

S-Nitrosothiols are unstable species. On the basis of published results (29), we assumed initially that decomposition in the dark would result in the metal-catalyzed conversion of 2 mol of GSNO to 1 mol of GSSG (with no formation of GS $^{\bullet}$ thiyl radicals) and 2 mol of NO. Hence, different molar ratios of GSSG and/or GSH were added to a solution of fresh GSNO and rHCaBP, but the level of protein S-glutathiolation (data not shown) never reached the level seen in Figure 1B. GSSG is not an effective S-glutathiolation agent as demonstrated by the presence of only unmodified rHCaBP in Figure 1C, where a 50-fold excess GSSG was added to the protein. Changing the pH [ammonium acetate buffer (pH 4) or ammonium bicarbonate buffer (pH 8)] or adding NO_x (formed on exposure of NO-saturated buffer to air) to fresh GSNO did not significantly alter the level of rHCaBP S-thiolation (data not shown). rHCaBP also was incubated with fresh GSNO in the presence and absence of bovine CuZnSOD or catalase to eliminate possible effects of O₂⁻ and H₂O₂, but no increase in the level of S-thiolation over that seen in Figure 1A was detected (data not shown).

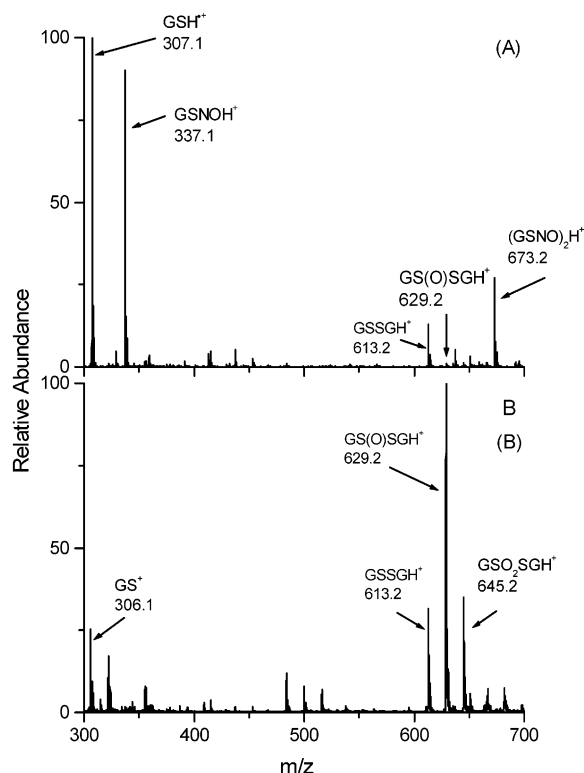


FIGURE 2: ESI mass spectra of (A) fresh GSNO and (B) decomposed GSNO. GSNO (5 mM) in water without added metal ion chelators was allowed to stand at room temperature in the dark for 0 h (fresh GSNO) and 63 h (decomposed GSNO). Samples were diluted into a 50% acetonitrile/0.2% formic acid mixture to a final concentration of $\sim 100 \mu\text{M}$, and directly infused into the Z-spray source of the QTOF2 mass spectrometer at a flow rate of $1 \mu\text{L}/\text{min}$. Experimental conditions are given in the legend of Figure 1.

Mechanism of GS(O)SG Formation. Li and co-workers (14) recently reported that GS(O)SG is a decomposition product of GSNO and a potent glutathiolating agent. Figure 2 compares the ESI mass spectra of fresh and decomposed GSNO solutions. The spectrum of fresh GSNO is dominated by peaks at m/z 307.1 and 337.1 (Figure 2A). The base peak at m/z 307.1 is assigned to GS^+ with a proton (GSH^+). Since this species has an odd number of nitrogen atoms (three) and an odd mass (307.1), it must be an odd-electron ion (30) that arises from GSNO homolysis ($\text{GSNO} \rightarrow \text{GS}^+ + \text{NO}^*$) and protonation in the ESI source. GS^+ dimerization followed by protonation would give rise to the relatively abundant peak at m/z 613.2 assigned to GSSGH^+ . The peaks at m/z 337 and 673 are assigned to the protonated ions (MH^+) of GSNO and its dimer, $(\text{GSNO})_2\text{H}^+$, respectively. There is also a minor peak at m/z 629 arising from the MH^+ ion of GS(O)SG, which is a decomposition product present in commercial GSNO. This ion dominates the spectrum of GSNO that was allowed to decompose over the course of 63 h in the dark. The peak at m/z 306 is assigned to GS^+ , which likely arises from heterolysis of GS(O)SG [$\text{GS(O)SG} + \text{H}^+ \rightarrow \text{GS}^+ + \text{GSOH}$] in the ESI source since no peak at m/z 306 is observed in the mass spectrum of fresh GSNO solutions (Figure 2A). Other abundant peaks are those at m/z 613 and 645 assigned to the MH^+ ions of GSSG and GSO_2SG , respectively, which are formed on GS(O)SG dimerization (see below).

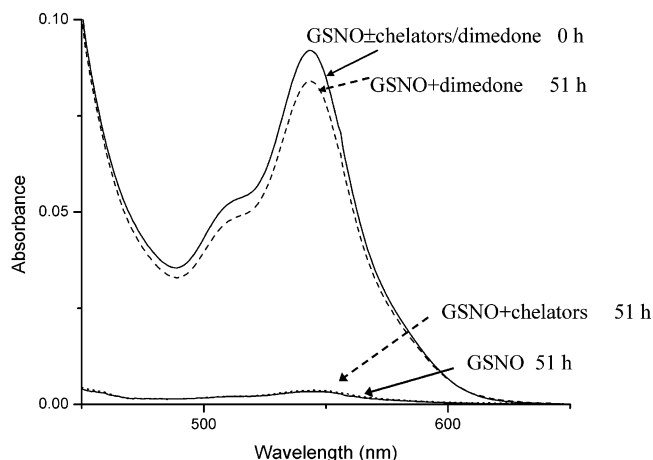


FIGURE 3: Effects of metal ion chelators and dimedone on the decomposition of 5 mM GSNO. Absorbance between 450 and 650 nm of GSNO in water after standing at room temperature in the dark for 0 h in the presence or absence of added reagents (top solid line), for 51 h in the presence of 10 mM dimedone (top dashed line), for 51 h in the presence of 200 μM neocuproine and 200 μM DTPA (bottom dotted line), and for 51 h in the absence of added reagents (bottom solid line). Spectra were recorded in a 1 cm cuvette at 25°C .

Although Li and co-workers (14) identified GS(O)SG as a potent S-glutathiolation agent, the mechanism of its formation from GSNO was not examined. Hence, GSNO decomposition was monitored in the presence of metal chelators (neocuproine and DTPA) and dimedone to probe the pathway of its conversion to GS(O)SG. RSNOs give rise to an absorption band centered at $\sim 335 \text{ nm}$ ($\epsilon = 890 \text{ cm}^{-1} \text{ M}^{-1}$) and a second, nearly electric-dipole-forbidden, band at $\sim 550 \text{ nm}$ ($\epsilon = 16 \text{ cm}^{-1} \text{ M}^{-1}$) (31). Since neocuproine and dimedone both absorb at 335 nm, the weak 550 nm band was used here to monitor GSNO decomposition. Decomposition of GSNO slowed dramatically when dimedone was present in solution, and an only $\sim 10\%$ loss of SNO absorbance was observed after 51 h (Figure 3). In contrast, the metal chelators had no effect on GSNO stability, indicating that GSNO decomposition in the dark over the course of 51 h is not a copper-catalyzed process (32).

Nitroxyl Scavenging. Metmyoglobin exhibits different spectral properties when the Fe^{III} in the protein binds different axial ligands in the distal cavity (33). Since metmyoglobin was shown to be an efficient scavenger of nitroxyl released from S-nitrosodithiothreitol (27), it was used here to probe the release of nitroxyl on GSNO hydrolysis. After incubation for 24 h in the dark of substoichiometric metmyoglobin with GSNO and dimedone, the Fe^{III} heme is fully converted to the nitrosyl form ($\text{Fe}^{\text{II}}\text{—NO}$) (Figure 4, top solid line). However, in the absence of dimedone, only a fraction of heme is transformed to the $\text{Fe}^{\text{II}}\text{—NO}$ form (Figure 4, dashed line). Interestingly, when metmyoglobin is present in solution, dimedone promotes GSNO decomposition (Figure 5, bottom solid line vs dashed line), whereas in the absence of metmyoglobin, dimedone strongly inhibits the breakdown of GSNO (Figure 3). These observations suggest that nitroxyl reacts with the GS—dimedone thioether to re-form GSNO as discussed below.

S-Glutathiolation of HCuZnSOD. Unlike rHCaBP, S-glutathiolated HCuZnSOD has been isolated from cells (16), and the structure of CuZnSOD from various sources has been

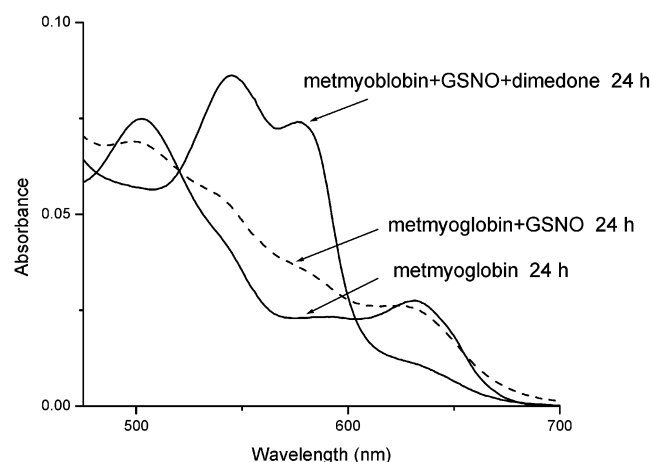


FIGURE 4: Conversion of metmyoglobin (Fe^{III}) to nitrosylmyoglobin ($\text{Fe}^{\text{II}}\text{-NO}$) by GSNO. GSNO (5 mM) and metmyoglobin (185 μM) were incubated in the presence (top solid line) or absence (dashed line) of 5 mM dimedone in water at 20 $^{\circ}\text{C}$ for 24 h under anaerobic conditions in the dark. The reaction solution was diluted 10-fold into degassed 100 mM potassium phosphate buffer (pH 7.0) in a sealed 0.4 cm cuvette just before the absorption spectrum was recorded. The bottom solid line is 18.5 μM metmyoglobin alone.

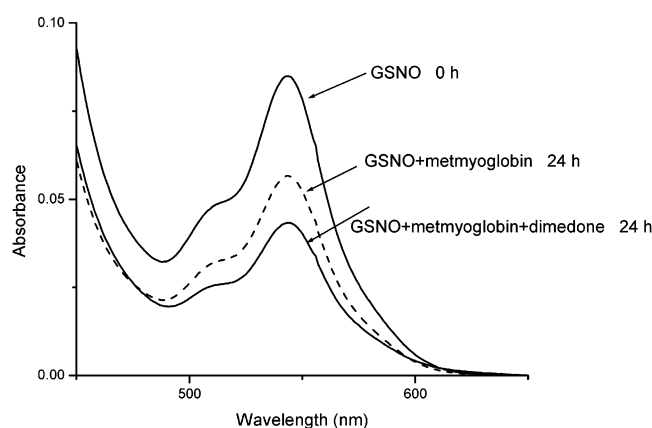


FIGURE 5: Effects of dimedone on the decomposition of GSNO in the presence of metmyoglobin. GSNO (5 mM) and metmyoglobin (185 μM) were incubated in the presence (bottom solid line) or absence (dashed line) of 5 mM dimedone in water at 20 $^{\circ}\text{C}$ for 24 h under anaerobic conditions in the dark. Metmyoglobin was removed by ultrafiltration before the absorbance of GSNO was recorded. The top solid line is freshly prepared 5 mM GSNO in water. Spectra were recorded in a 1 cm cuvette.

determined to high resolution (34–36). Thus, S-glutathiolation of HCuZnSOD by decomposed GSNO was investigated in an effort to provide insight into why certain cysteine residues are S-glutathiolated *in vivo*. DTNB titration revealed ~ 0.15 free thiol per HCuZnSOD dimer, and its ESI mass spectrum uncovered two major components (Figure 6A). The lighter component corresponds to the unmodified metal-free or apoHCuZnSOD monomer (theoretical mass of 15 844.6 Da), and the heavier component ($M + 32$ Da) is assigned to the apoHCuZnSOD monomer with a bound S^0 atom. Briggs and co-workers showed that sulfhydryl groups in HCuZnSOD react with zero-valent sulfur during the purification procedure to yield a product with a 325 nm absorption band (37) that is seen in the inset of Figure 6 (solid line).

The 325 nm absorption disappears after HCuZnSOD is incubated with DTT (Figure 6A inset, dashed line), as does the $M + 32$ Da peak in the mass spectrum (Figure 6B).

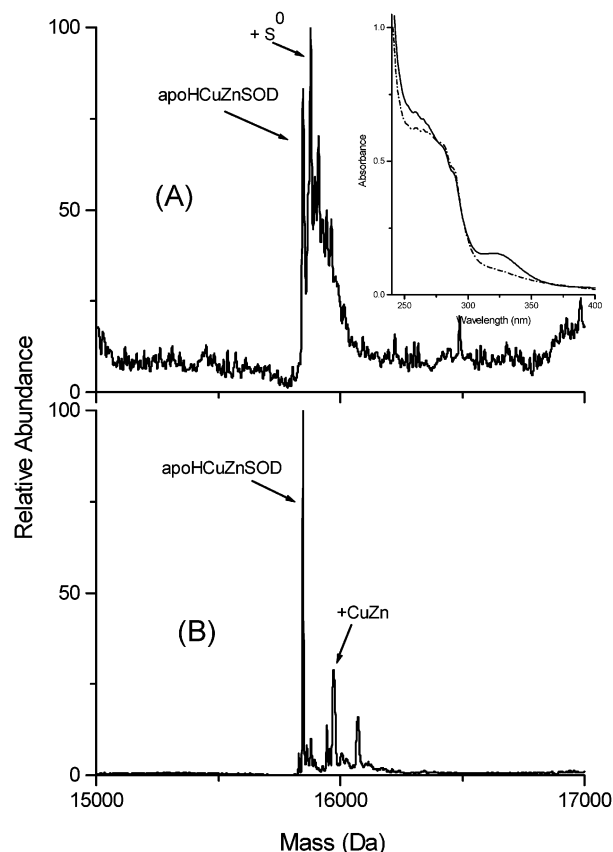


FIGURE 6: Deconvoluted ESI mass spectra of HCuZnSOD: (A) untreated HCuZnSOD and (B) DTT-reduced HCuZnSOD. The arrows point to peaks at 15 845, 15 877, and 15 974 Da corresponding to the metal-free (apoHCuZnSOD), the S^0 -derivatized metal-free ($+\text{S}^0$), and the metal-loaded ($+\text{CuZn}$) protein monomer, respectively. Experimental conditions are given in the legend of Figure 1. The inset shows UV-vis absorption of HCuZnSOD in 50 mM ammonium bicarbonate buffer (pH 7.8) at room temperature in a 1 cm cuvette: (—) 66 μM untreated HCuZnSOD and (---) 61 μM DTT-reduced HCuZnSOD.

Moreover, a peak at $M + 129$ Da is uncovered in the mass spectrum of the DTT-reduced protein (Figure 6B), and is assigned to a monomer with one Zn (65.4 units) and one Cu (63.5 units) bound. Peaks corresponding to the metal-loaded monomer are also seen in Figure 7. Reduced HCuZnSOD was incubated with fresh and decomposed GSNO, but only the latter is an effective glutathiolating agent (panel A vs panel B of Figure 7). This mirrors the results obtained for rHcBP (panel A vs panel B of Figure 1), although the yield of rHcBP glutathiolation is greater than that of HCuZnSOD (Figure 1B vs Figure 7B). The yield of glutathiolated HCuZnSOD was smaller in Tris-HCl buffer (pH 7.4) (data not shown) compared to that in ammonium acetate buffer (pH 4.0) (Figure 7). Additionally, GSSG does not effectively glutathiolate HCuZnSOD (data not shown).

Identification of the Modification Site on HCuZnSOD. To identify the glutathiolated amino acid residue, tryptic digests of HCuZnSOD were analyzed by MALDI-TOF. Although the sequence coverage was only $\sim 42\%$ (Table 1), the peptide mass fingerprints revealed that the DGVADVSIEDSVISLS-GDHCIGR peptide (D93–R116) has an increased mass of 305 Da in the sample exposed to decomposed GSNO (panel A vs panel B of Figure 8). Since this is consistent with the addition of a single GS group, as observed for intact HCuZnSOD (Figure 7), Cys111 in the D93–R116 peptide

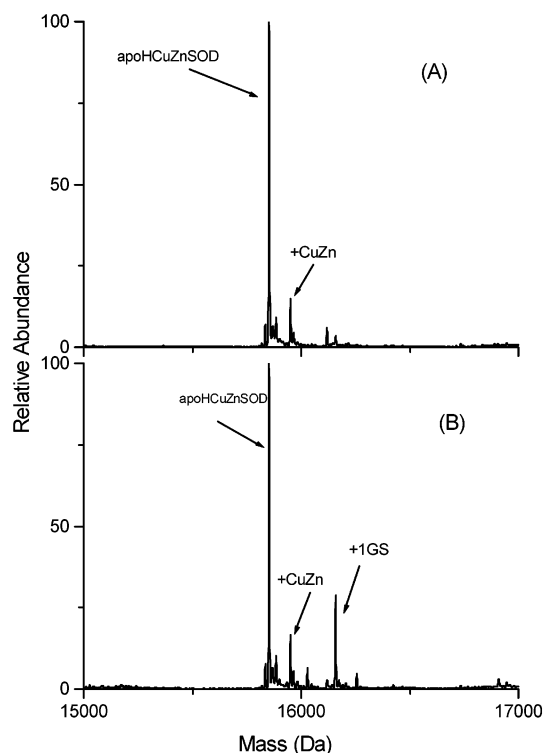


FIGURE 7: Effects of GSNO on the S-glutathiolation of HCUZnSOD. Deconvoluted ESI mass spectra of DTT-reduced HCUZnSOD following incubation of 66 μ M protein with a 100-fold molar excess of (A) fresh GSNO and (B) decomposed GSNO in 50 mM ammonium acetate buffer (pH 4) for 30 min at 37 °C in the dark. The arrows point to peaks with masses of 15 845, 15 974, and 16 150 Da corresponding to the metal-free (apoHCUZnSOD), metal-loaded (+CuZn), and singly S-glutathiolated metal free (+1GS) protein monomer, respectively. Experimental conditions are given in the legend of Figure 1.

is identified as the likely site of S-glutathiolation. Moreover, a peak at m/z 2489 corresponding to the MH^+ ion of the D93–R116 peptide with an increased mass of 32 Da is present in the mass fingerprints of the digests of both untreated HCUZnSOD and reduced HCUZnSOD that was exposed to decomposed GSNO (Figure 8). A comparison of panels A and B of Figure 8 indicates that the peak corresponding to the D93–R116 peptide with S^0 (m/z 2489) is much less intense than the D93–R116 peak (m/z 2457) following reduction of HCUZnSOD. Hence, Cys111 is also likely the residue that is linked to the single zero-valent sulfur atom found in HCUZnSOD. Although linking of an S^0 atom to the extra sulfhydryl in HCUZnSOD was suggested more than 20 years ago (37, 38), the evidence provided in Figure 8 is the first to support this assignment.

S-Glutathiolation of GAPDH. The effects of fresh and decomposed GSNO on GAPDH are also of interest since it was found to be a target for S-glutathiolation *in vivo* and *in vitro* following exposure to oxidative stress (10, 19, 39, 40). Thus, examination of S-glutathiolation of rabbit muscle GAPDH, a homotetramer (41), was carried out to provide further insight into protein S-glutathiolation *in vitro* and *in vivo*. GAPDH was incubated with a 50-fold molar ratio of fresh or decomposed GSNO for 20 min at room temperature. The mass spectrum of GAPDH exposed to fresh GSNO (Figure 9A) shows a major peak at 35 691 Da, which corresponds to the reported mass of the monomer (42), and minor peaks at $M + 32$ Da and $M + 305$ Da (+1GS). The

singly GS-labeled monomer is the major species in the mass spectrum following exposure to decomposed GSNO (Figure 9B). Additionally, a peak at $M + 610$ Da (+2GS) is observed in Figure 9B. Therefore, GAPDH is glutathiolated to a much greater extent in decomposed than in fresh GSNO solutions (panel A vs panel B of Figure 9). The $M + 32$ Da species, which is also present in untreated GAPDH samples (data not shown), has not been identified but may result from addition of two oxygen atoms to the GAPDH monomer. Exposure to fresh or decomposed GSNO does not appear to alter the relative abundance of the $M + 32$ Da species (Figure 9).

S-Glutathiolation of BSA. Serum albumin is the most abundant protein in plasma and is proposed to have an antioxidant role (21). Hence, it is of interest to establish if this protein is S-glutathiolated in decomposed GSNO solutions on its single free cysteine residue, Cys34. The mass spectrum of BSA after the commercial protein was dialyzed against MilliQ water shows a major peak at 66 430 Da (Figure 10A), which corresponds to the reported mass of the protein (43). Singly GS-labeled BSA is the major species in the mass spectrum (Figure 10B) after the DTT-reduced protein was exposed to a 100-fold molar excess of decomposed GSNO for 20 min at room temperature.

DISCUSSION

Protein S-glutathiolation has been observed *in vivo* and *in vitro* (3, 4, 8, 44). This oxidative modification is recognized as one of the physiological responses to nitrosative and oxidative stress, but how proteins are S-glutathiolated *in vivo* is not clear. GSH alone reportedly does not S-glutathiolate proteins such as cathepsin (9) and GAPDH (10), and protein S-thiolation occurred without GSSG in neutrophil-treated hepatocytes (4). It has been deduced that S-glutathiolation of proteins by GSSG *in vivo* likely is not an efficient process (14). Clearly, GSSG is not an effective S-glutathiolating agent of rHcBP (Figure 1C) and HCUZnSOD (data not shown) *in vitro*, consistent with observations on glycogen phosphorylase *b* (8) and aldose reductase (11). Recently, it was reported that GSNO S-glutathiolates proteins *in vivo* and *in vitro* (5, 8–12, 40), but the results presented here reveal that decomposed GSNO solutions contain a much more effective S-glutathiolating reagent for rHcBP, HCUZnSOD, and GAPDH than fresh solutions (Figures 1, 7, and 9). Similar results were obtained by Li *et al.* for neurogranin and neuromodulin (14) and by Ji *et al.* for glycogen phosphorylase *b* (8). Interestingly, the formation of the P–SSG species did not lead to the detection here of cross-linked protein (P–SS–P) in any of the mass spectra that were recorded.

GS(O)SG, a GSNO decomposition product (Figure 2), was suggested to be a potent S-glutathiolating agent for proteins (14). However, it is not clear from the published work on protein S-glutathiolation triggered by GSNO whether NO or GSNO plays a role since residual GSNO was present in the decomposed GSNO solutions (14). Also, the mechanism of GSNO decomposition to GS(O)SG has not been determined, although Huang and Huang (45) speculated that GSNO decomposition was likely catalyzed by copper ions.

In the work presented here, GSNO decomposition in the dark was monitored by the loss of its SNO absorption at

Table 1: Tryptic Peptides in the MALDI Mass Fingerprint of S-Glutathiolated HCuZnSOD^a

residues	peptide sequence	observed MH ⁺ ^b	calculated MH ⁺ ^c	chemical modification ^d
117–123	TLVVHEK	825.3	825.5	
38–46	GLTEGLHGF	930.4	930.5	
81–92	HVGDLGNVTADK	1225.5	1225.6	
11–24	GDGPVQGIINFEQK	1501.6	1501.8	
93–116	DGVADVSIEDSVISLSGDHCIIGR	2457.4	2457.2	
93–116	DGVADVSIEDSVISLSGDH $\dot{\text{C}}$ IIGR	2489.7	2489.3	S ⁰
93–116	DGVADVSIEDSVISLSGDH $\dot{\text{C}}$ IIGR	2762.6	2762.2	GS

^a HCuZnSOD was incubated with a 100-fold molar excess of decomposed GSNO in 50 mM ammonium acetate buffer (pH 4.0) for 30 min at 37 °C. Tryptic digestion was carried out as described in Materials and Methods, and the tryptic peptides were analyzed by MALDI-TOF MS.

^b Observed monoisotopic masses of the singly protonated ions (MH⁺) of the tryptic peptides. ^c Calculated monoisotopic masses of the MH⁺ ions of the tryptic peptides. ^d Chemical modification of Cys111 based on the mass shift in the D93–R116 peptide (see the text).

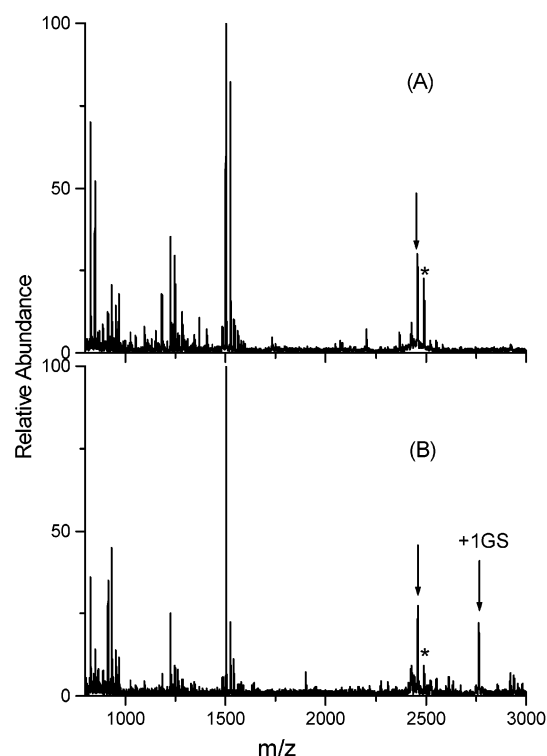


FIGURE 8: MALDI-TOF mass fingerprints of the tryptic digests of HCuZnSOD: (A) untreated HCuZnSOD and (B) DTT-reduced HCuZnSOD following incubation with decomposed GSNO. The arrows point to peaks at m/z 2457.4 and 2762.6 corresponding to unmodified and GS-derivatized D93–R116 peptides, respectively. The asterisk denotes the peak at m/z 2489.7 of the S⁰-derivatized D93–R116 peptide. Cys111 is assumed to be the site of derivatization in each case (see Table 1).

335 nm (Figure 1A, inset). A GSNO decomposition product is an efficient protein S-glutathiolation agent (Figures 1B, 7B, 9B, and 10B) in the absence of any detectable GSNO (Figure 2B). On the other hand, in fresh GSNO solutions containing only a trace of GS(O)SG as monitored by ESI-MS (Figure 2A), little S-glutathiolation of rHcBP, HCuZnSOD, and GAPDH occurred (Figures 1A, 7A, and 9A). Moreover, addition of solutions of NO_x from aerobic NO decomposition (NO → NO_x) did not alter the extent of rHcBP S-glutathiolation (data not shown). These results indicate that neither GSNO nor NO_x is directly involved in S-glutathiolation of rHcBP, HCuZnSOD, or GAPDH *in vitro*.

As reported by Li *et al.* (14), the major decomposition products of GSNO were found to be GS(O)SG, GSO₂SG, and GSSG (Figure 2B). How is GSNO converted to these

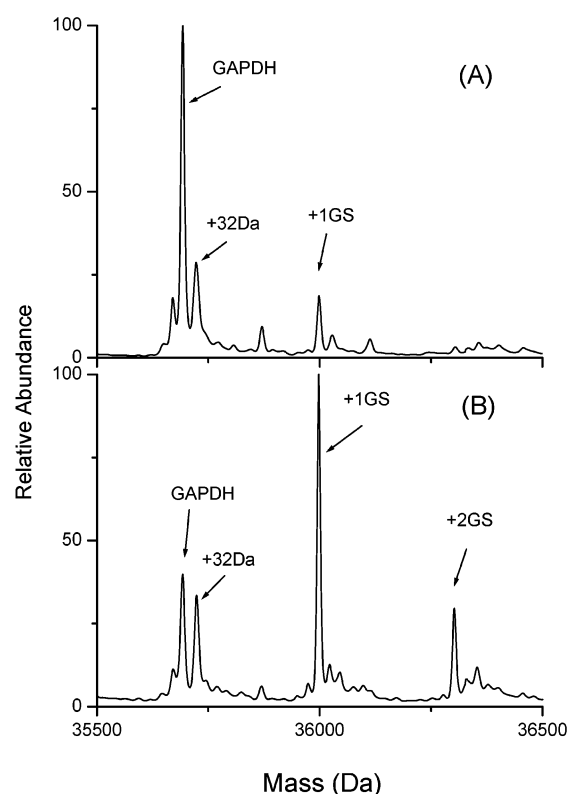
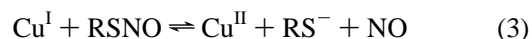


FIGURE 9: Effects of GSNO on the S-glutathiolation of GAPDH. Deconvoluted ESI mass spectra of the GAPDH monomer after incubation with a 50-fold molar excess of (A) fresh GSNO and (B) decomposed GSNO in 50 mM Tris-HCl buffer (pH 7.4) for 20 min at room temperature in the dark. The arrows point to peaks at 35 691 (M), M + 32, M + 305, and M + 610 Da corresponding to unmodified (GAPDH), possibly oxidized (+32 Da), and singly (+1GS) and doubly (+2GS) GS-labeled protein monomer, respectively. Experimental conditions are given in the legend of Figure 1.

products? Thermal and photochemical homolysis pathways have been proposed for RSNO decomposition (46):



Also, copper-catalyzed reductive cleavage (eqs 2 and 3) results in the rapid breakdown of many RSNOs at ambient temperature in the dark, under which conditions homolysis (eq 1) is highly inefficient (47).



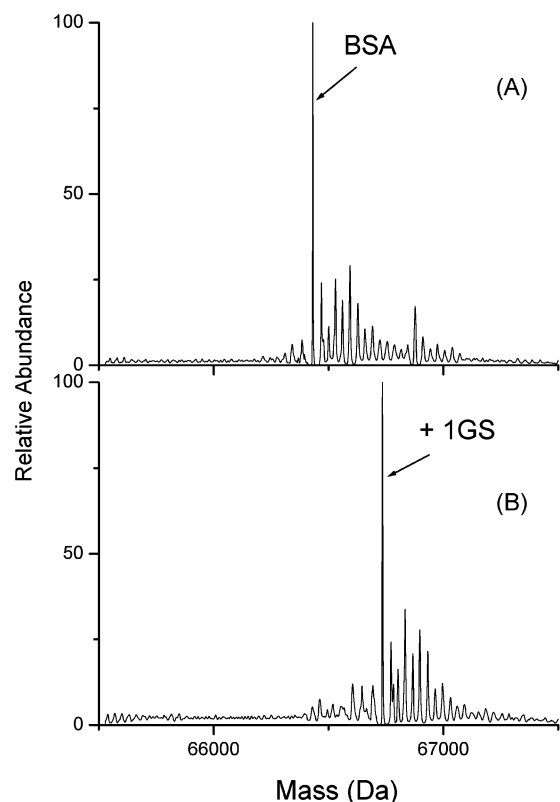
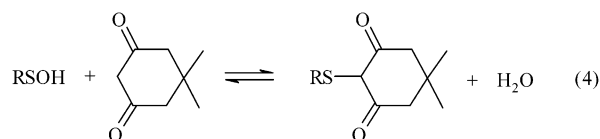


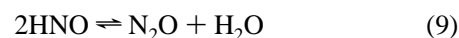
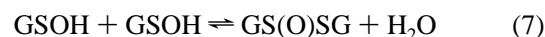
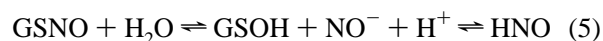
FIGURE 10: BSA S-glutathiolation by decomposed GSNO. Deconvoluted ESI mass spectra of (A) DTT-reduced BSA and (B) DTT-reduced BSA following incubation with a 100-fold molar excess of decomposed GSNO in 100 mM Tris-HCl buffer (pH 7.4) for 20 min at room temperature in the dark. The arrows point to peaks at 66 430 and 66 735 Da corresponding to unmodified and singly GS-labeled (+1GS) BSA, respectively. Samples for MS analysis were exchanged into water by dialysis, added to a 20% methanol/5% acetic acid mixture to a final protein concentration of 5–10 μ M, and directly infused into the Z-spray source of the QTOF2 instrument. Experimental conditions are given in the legend of Figure 1.

Figure 3 shows that the presence of dimedone, but not metal chelators, prevents GSNO decomposition. Thus, metal ions are not involved in GSNO decomposition under the conditions used here. This is consistent with the results of Williams and co-workers (47), who have shown that copper-catalyzed decomposition is efficient at low GSNO concentrations ($\sim 3 \mu$ M) but is prevented at high concentrations due to product inhibition. The GSSG produced on copper-catalyzed GSNO breakdown (eq 2) forms a stable Cu^{II} chelate and inhibits further redox turnover of the metal (eq 3) required for catalytic GSNO cleavage (47).

Dimedone has been shown to react specifically with sulfenic acids to form a stable thioether product (9, 48):

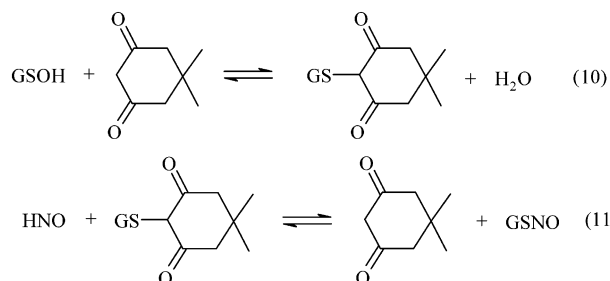


Since dimedone is a scavenger of GSOH and strongly inhibits GSNO breakdown (Figure 3C), the following mechanism for GS(O)SG formation from GSNO is proposed:



In this scheme, GSNO hydrolysis generates GSOH and HNO/NO^- (eq 5). GSOH further reacts with GSNO to give GS(O)SG and HNO/NO^- (eq 6). GSOH can also undergo self-condensation (49) to yield GS(O)SG (eq 7), which dimerizes to yield GSO_2SG and GSSG as products (eq 8) (50). Presumably, reaction 5 is rate-limiting, and reactions 6 and 7 drive GSNO breakdown by consuming GSOH.

When dimedone is present, it traps GSOH (eq 10) and prevents its further reaction with GSNO (eq 6) or self-condensation (eq 7). However, since <10% of GSNO is consumed in the presence of dimedone (Figure 3), most of the thioether formed in reaction 10 must be reconverted to GSNO. The rate of reaction 9, which removes HNO from solution by dimerization and dehydration, is dependent on the square of the HNO concentration. Trapping of GSOH by dimedone will decrease the HNO concentration by inhibiting reaction 6, and nitroxyl attack on the GS–dimedone thioether to re-form GSNO (eq 11) will be favored over HNO dimerization (eq 9). Breakdown of thiol–dimedone adducts has been previously detected by Benitez *et al.* (51) under acidic conditions.



To obtain further evidence that HNO/NO^- is released upon GSNO decomposition, metmyoglobin was added as a nitroxyl scavenger (27). In the presence of dimedone, metmyoglobin was fully converted into its nitrosyl ($\text{Fe}^{\text{II}}\text{--NO}$) form (Figure 4, solid line), confirming that nitroxyl is released on GSNO hydrolysis. Moreover, dimedone inhibits GSNO consumption in the absence (Figure 3) but *not* in the presence of metmyoglobin (Figure 5, bottom solid line), revealing that nitroxyl scavenging prevents regeneration of GSNO as predicted (eq 11). However, GSOH is free to react with GSNO (eq 6) when dimedone is absent, and the lower scavenging yield under this condition (Figure 4) probably reflects an increased rate of HNO dimerization (eq 9).

GS(O)SG formed on GSNO decomposition reacts with free thiols such as GSH and certain protein thiols (PSH) (14):



GSOH produced *in situ* in reaction 12 may act also as a protein S-glutathiolating agent (9) depending on the relative rates of reactions 7 and 13.



No GSOH was detected here in the decomposed GSNO solutions by mass spectrometry, which is consistent with the known instability of sulfenic acids to dimerization and dehydration (49) (reaction 7). Interestingly, many of the proteins that are susceptible to mixed disulfide formation in response to nitrosative stress (3) have been reported to undergo S-thiolation under oxidative conditions (10, 52–54). What determines the susceptibility of protein thiols to S-glutathiolation? For example, of the five free cysteine residues in rHcCaBP, S-glutathiolation of Cys187 is preferred (15). Since the structure of rHcCaBP is not yet known, HcCuZnSOD was chosen as another model protein in this study. CuZnSODs from different species possess three conserved cysteine residues per monomer (16). Two of them form an intrasubunit disulfide bridge, and the side chain of the third highly conserved cysteine points toward the interior of the protein. In addition to the conserved cysteines, a few CuZnSODs possess exposed free thiols, termed extra sulfhydryl or extra cysteine residues. HcCuZnSOD is among the extra-cysteine-containing enzymes. The extra Cys111 causes the observed heterogeneity of HcCuZnSOD preparations since it is derivatized in both the wild-type and recombinant protein (55, 56). Cys111 is also the site modified naturally or artificially by mixed disulfide formation with free cysteine or glutathione (57, 58).

Here we report that the D93–R116 peptide, which contains Cys111, is labeled with the single zero-valent sulfur atom found in commercial HcCuZnSOD preparations. Cys111 is also the site of S-glutathiolation (Figure 8). However, the yield of S-glutathiolated HcCuZnSOD is much lower than that of rHcCaBP (Figure 1B vs Figure 7B), but comparable to that of the enzyme isolated from cells (17, 18). Liu *et al.* (57) found that only ~50% of HcCuZnSOD was modified by 4-vinylpyridine or DTNB, although a 100- or 1000-fold molar excess of reagent over protein sulfhydryl was employed. Cys111 is near the dimer interface, and the distance between the two sulfhydryl groups is ~10 Å as estimated from the crystal structure of HcCuZnSOD (59). Because of their proximity (57), modification of Cys111 on one subunit of the dimer likely impedes access of the modifying reagent to Cys111 on the other subunit. The yield of S-glutathiolated HcCuZnSOD at pH 4.0 (Figure 5B) was higher than that at pH 7.4 (data not shown), which suggests that HcCuZnSOD has greater conformational flexibility at lower pHs, making Cys111 more accessible.

GAPDH is a homotetramer, and each monomer contains four free cysteine residues. On the basis of DTNB reactivity, the four thiols have been classified into three groups: one fast reacting thiol, which is most likely the active site Cys149 (60–62); one thiol that reacts at an intermediate rate; and two slow reacting thiols (60, 63). GAPDH is found to be S-glutathiolated by decomposed GSNO to a large extent on one cysteine and to a lesser extent on a second cysteine (Figure 9B). After S-glutathiolation, ~90% of the GAPDH activity is lost (data not shown), so it is likely that the active site Cys149 is S-glutathiolated. The cysteine residue with lower GS(O)SG reactivity is probably that with intermediate DTNB reactivity.

BSA has 35 cysteine residues, but 34 are involved in disulfide bridges. Only Cys34 possesses a free thiol that can

partake in thiol-specific reactions (21, 64). *In vivo*, Cys34 is in the free thiol form, but once extracted and purified from plasma, it is partially involved in intermolecular disulfide bond formation or in mixed disulfides with other low-molecular weight thiols (21). Here we report that DTT-reduced BSA, which possesses 0.86 free thiol per molecule, undergoes a mass increase of 305 Da on incubation with decomposed GSNO (Figure 10B). This indicates that BSA is efficiently S-glutathiolated by GS(O)SG presumably on Cys34.

The active site structure of the GAPDH tetramer is conserved (65). The distance between two active site Cys149 side chains in *Bacillus stearothermophilus* GAPDH is ~35 Å (66), which is much larger than the separation of ~10 Å between the Cys111 residues in HcCuZnSOD. Also, the X-ray structure of human serum albumin (67) showed that Cys34 is partially solvent exposed. Therefore, accessibility to the glutathiolating reagent and a cavity that can accommodate the GS group are likely prerequisites for protein S-glutathiolation. Although no structural properties that render accessible protein sulfhydryls equally reactive to S-glutathiolation have been identified (1), cysteines with depressed pK_a values because of their proximity to basic amino acid residues are preferentially S-glutathiolated. Examples include Cys298 in aldose reductase and Cys269 in c-Jun (11, 40).

CONCLUSIONS

GS(O)SG is an efficient S-glutathiolation reagent unlike GSNO, GSH, or GSSG. GS(O)SG can be formed by the treatment of GSH with H_2O_2 (68), by bubbling GSH or GSSG solutions with NO gas (14), and from decomposed GSNO. Interestingly, GS(O)SG was found to be present at low levels in rat brain slices, and its concentration increased under oxidative stress (14). Thus, oxidative or nitrosative stress may promote protein S-glutathiolation *in vivo*, with GS(O)SG acting as a thiolating agent in this process. It is also possible that the slow GSNO hydrolysis to GSOH observed here is enzymatically catalyzed *in vivo*, but such activity remains to be identified.

ACKNOWLEDGMENT

We thank David Yong-Hoi Yeung and Biao Shen for their assistance with the preparation of rHcCaBP and BSA. Lekha Sleno and Dominic Cuerrier are thanked for helpful discussions about GAPDH modification.

REFERENCES

1. Thomas, J. A., Poland, B., and Honzatko, R. (1995) Protein sulfhydryls and their role in the antioxidant function of protein S-thiolation, *Arch. Biochem. Biophys.* 319, 1–9.
2. Ward, N. E., Stewart, J. R., Ioannides, C. G., and O'Brian, C. A. (2000) Oxidant-induced S-glutathiolation inactivates protein kinase C- α (PKC- α): a potential mechanism of PKC isozyme regulation, *Biochemistry* 39, 10319–10329.
3. Klatt, P., and Lamas, S. (2000) Regulation of protein function by S-glutathiolation in response to oxidative and nitrosative stress, *Eur. J. Biochem.* 267, 4928–4944.
4. Chai, Y. C., Hendrich, S., and Thomas, J. A. (1994) Protein S-thiolation in hepatocytes stimulated by *tert*-butyl hydroperoxide, menadione, and neutrophils, *Arch. Biochem. Biophys.* 310, 264–272.
5. Padgett, C. M., and Whorton, A. R. (1998) Cellular responses to nitric oxide: role of protein S-thiolation/dethiolation, *Arch. Biochem. Biophys.* 358, 232–242.

6. Gilbert, H. F. (1990) Molecular and cellular aspects of thiol-disulfide exchange, *Adv. Enzymol. Relat. Areas Mol. Biol.* 63, 69–172.
7. Park, E. M., and Thomas, J. A. (1988) S-Thiolation of creatine kinase and glycogen phosphorylase *b* initiated by partially reduced oxygen species, *Biochim. Biophys. Acta* 964, 151–160.
8. Ji, Y., Akerboom, T. P., Sies, H., and Thomas, J. A. (1999) S-Nitrosylation and S-glutathiolation of protein sulfhydryls by S-nitroso glutathione, *Arch. Biochem. Biophys.* 362, 67–78.
9. Percival, M. D., Ouellet, M., Campagnolo, C., Claveau, D., and Li, C. (1999) Inhibition of cathepsin K by nitric oxide donors: evidence for the formation of mixed disulfides and a sulfenic acid, *Biochemistry* 38, 13574–13583.
10. Mohr, S., Hallak, H., Boitte, A., Lapetina, E. G., and Brune, B. (1999) Nitric oxide-induced S-glutathionylation and inactivation of glyceraldehyde-3-phosphate dehydrogenase, *J. Biol. Chem.* 274, 9427–9430.
11. Chandra, A., Srivastava, S., Petrash, J. M., Bhatnagar, A., and Srivastava, S. K. (1997) Modification of aldose reductase by S-nitrosoglutathione, *Biochemistry* 36, 15801–15809.
12. Zech, B., Wilm, M., Eldik, R. V., and Brune, B. (1999) Mass spectrometric analysis of nitric oxide-modified caspase-3, *J. Biol. Chem.* 274, 20931–20936.
13. Xian, M., Chen, X., Liu, Z., Wang, K., and Wang, P. G. (2000) Inhibition of papain by S-nitrosothiols. Formation of mixed disulfides, *J. Biol. Chem.* 275, 20467–20473.
14. Li, J., Huang, F. L., and Huang, K. P. (2001) Glutathiolation of proteins by glutathione disulfide S-oxide derived from S-nitrosoglutathione. Modifications of rat brain neurogranin/RC3 and neuromodulin/GAP-43, *J. Biol. Chem.* 276, 3098–3105.
15. Tao, L., Murphy, M. E., and English, A. M. (2002) S-Nitrosation of Ca²⁺-loaded and Ca²⁺-free recombinant calbindin D_{28K} from human brain, *Biochemistry* 41, 6185–6192.
16. Schinina, M. E., Carlini, P., Polticelli, F., Zappacosta, F., Bossa, F., and Calabrese, L. (1996) Amino acid sequence of chicken Cu, Zn-containing superoxide dismutase and identification of glutathionyl adducts at exposed cysteine residues, *Eur. J. Biochem.* 237, 433–439.
17. Marklund, S. L., Andersen, P. M., Forsgren, L., Nilsson, P., Ohlsson, P. I., Wikander, G., and Oberg, A. (1997) Normal binding and reactivity of copper in mutant superoxide dismutase isolated from amyotrophic lateral sclerosis patients, *J. Neurochem.* 69, 675–681.
18. Nakanishi, T., Kishikawa, M., Miyazaki, A., Shimizu, A., Ogawa, Y., Sakoda, S., Ohi, T., and Shoji, H. (1998) Simple and defined method to detect the SOD-1 mutants from patients with familial amyotrophic lateral sclerosis by mass spectrometry, *J. Neurosci. Methods* 81, 41–44.
19. Schuppe-Koistinen, I., Moldeus, P., Bergmann, T., and Cotgreave, I. A. (1994) S-Thiolation of human endothelial cell glyceraldehyde-3-phosphate dehydrogenase after hydrogen peroxide treatment, *Eur. J. Biochem.* 221, 1033–1037.
20. Eaton, P., Byers, H. L., Leeds, N., Ward, M. A., and Shattock, M. J. (2002) Detection, quantitation, purification, and identification of cardiac proteins S-thiolated during ischemia and reperfusion, *J. Biol. Chem.* 277, 9806–9811.
21. Carballal, S., Radi, R., Kirk, M. C., Barnes, S., Freeman, B. A., and Alvarez, B. (2003) Sulfenic acid formation in human serum albumin by hydrogen peroxide and peroxyxynitrite, *Biochemistry* 42, 9906–9914.
22. Halliwell, B. (1988) Albumin: an important extracellular antioxidant? *Biochem. Pharmacol.* 37, 569–571.
23. Halliwell, B., and Gutteridge, J. M. (1990) The antioxidants of human extracellular fluids, *Arch. Biochem. Biophys.* 280, 1–8.
24. Riddles, P. W., Blakeley, R. L., and Zerner, B. (1983) Reassessment of Ellman's reagent, *Methods Enzymol.* 91, 49–60.
25. Chen, Y. H., He, R. Q., Liu, Y., Liu, Y., and Xue, Z. G. (2000) Effect of human neuronal tau on denaturation and reactivation of rabbit muscle D-glyceraldehyde-3-phosphate dehydrogenase, *Biochem. J.* 351, 233–240.
26. Mathews, W. R., and Kerr, S. W. (1993) Biological activity of S-nitrosothiols: the role of nitric oxide, *J. Pharmacol. Exp. Ther.* 267, 1529–1537.
27. Arnelo, D. R., and Stamler, J. S. (1995) NO⁺, NO, and NO⁻ donation by S-nitrosothiols: implications for regulation of physiological functions by S-nitrosylation and acceleration of disulfide formation, *Arch. Biochem. Biophys.* 318, 279–285.
28. Kurahashi, T., Miyazaki, A., Suwan, S., and Isobe, M. (2001) Extensive investigations on oxidized amino acid residues in H₂O₂-treated Cu,Zn-SOD protein with LC-ESI-Q-TOF-MS, MS/MS for the determination of the copper-binding site, *J. Am. Chem. Soc.* 123, 9268–9278.
29. Singh, R. J., Hogg, N., Joseph, J., and Kalyanaraman, B. (1996) Mechanism of nitric oxide release from S-nitrosothiols, *J. Biol. Chem.* 271, 18596–18603.
30. McLafferty, F. W., Turecek, F., and Choi, J. (1996) *Interpretation of Mass Spectra*, 4th ed., University Science Books, Sausalito, CA.
31. Mohnney, B. K., and Walker, G. C. (1997) Conformational restriction of cysteine-bound NO in bovine serum albumin revealed by circular dichroism, *J. Am. Chem. Soc.* 119, 9311–9312.
32. Williams, D. L. H. (1999) The Chemistry of S-Nitrosothiols, *Acc. Chem. Res.* 32, 869–876.
33. Antonini, E., and Brunori, M. (1971) *Hemoglobin and myoglobin in their reactions with ligands*, North-Holland, Amsterdam.
34. Djinnovic, K., Gatti, G., Coda, A., Antolini, L., Pelosi, G., Desideri, A., Falconi, M., Marmocchi, F., Rotilio, G., and Bolognesi, M. (1992) Crystal structure of yeast Cu,Zn superoxide dismutase. Crystallographic refinement at 2.5 Å resolution, *J. Mol. Biol.* 225, 791–809.
35. Tainer, J. A., Getzoff, E. D., Beem, K. M., Richardson, J. S., and Richardson, D. C. (1982) Determination and analysis of the 2 Å structure of copper, zinc superoxide dismutase, *J. Mol. Biol.* 160, 181–217.
36. Parge, H. E., Hallewell, R. A., and Tainer, J. A. (1992) Atomic structures of wild-type and thermostable mutant recombinant human Cu,Zn superoxide dismutase, *Proc. Natl. Acad. Sci. U.S.A.* 89, 6109–6113.
37. Briggs, R. G., and Fee, J. A. (1978) Sulfhydryl reactivity of human erythrocyte superoxide dismutase. On the origin of the unusual spectral properties of the protein when prepared by a procedure utilizing chloroform and ethanol for the precipitation of hemoglobin, *Biochim. Biophys. Acta* 537, 100–109.
38. Calabrese, L., Federici, G., Bannister, W. H., Bannister, J. V., Rotilio, G., and Finazzi-Agro, A. (1975) Labile sulfur in human superoxide dismutase, *Eur. J. Biochem.* 56, 305–309.
39. Ravichandran, V., Seres, T., Moriguchi, T., Thomas, J. A., and Johnston, R. B. (1994) S-Thiolation of glyceraldehyde-3-phosphate dehydrogenase induced by the phagocytosis-associated respiratory burst in blood monocytes, *J. Biol. Chem.* 269, 25010–25015.
40. Klatt, P., Pineda Molina, E., Perez-Sala, D., and Lamas, S. (2000) Novel application of S-nitrosoglutathione-Sepharose to identify proteins that are potential targets for S-nitrosoglutathione-induced mixed-disulfide formation, *Biochem. J.* 349, 567–578.
41. Applequist, S. E., Keyna, U., Calvin, M. R., Beck-Engeser, G. B., Raman, C., and Jack, H. M. (1995) Sequence of the rabbit glyceraldehyde-3-phosphate dehydrogenase-encoding cDNA, *Gene* 163, 325–326.
42. Rivera-Nieves, J., Thompson, W. C., Levine, R. L., and Moss, J. (1999) Thiols mediate superoxide-dependent NADH modification of glyceraldehyde-3-phosphate dehydrogenase, *J. Biol. Chem.* 274, 19525–19531.
43. Hirayama, K., Akashi, S., Furuya, M., and Fukuhara, K. (1990) Rapid confirmation and revision of the primary structure of bovine serum albumin by ESIMS and Frit-FAB LC/MS, *Biochem. Biophys. Res. Commun.* 173, 639–646.
44. Schuppe-Koistinen, I., Gerdes, R., Moldeus, P., and Cotgreave, I. A. (1994) Studies on the reversibility of protein S-thiolation in human endothelial cells, *Arch. Biochem. Biophys.* 315, 226–234.
45. Huang, K. P., and Huang, F. L. (2002) Glutathionylation of proteins by glutathione disulfide S-oxide, *Biochem. Pharmacol.* 64, 1049–1056.
46. Butler, A. R., and Williams, D. L. H. (1993) The physiological role of nitric oxide, *Chem. Soc. Rev.* 22, 233–241.
47. Noble, D. R., and Williams, D. L. (2000) Structure–reactivity studies of the Cu²⁺-catalyzed decomposition of four S-nitrosothiols based around the S-Nitrosocysteine/S-nitrosoglutathione structures, *Nitric Oxide* 4, 392–398.
48. Allison, W. S. (1976) Formation and reactions of sulfenic acids in proteins, *Acc. Chem. Res.* 9, 293–299.
49. Davis, F. A., Jenkins, L. A., and Billmers, R. L. (1986) Chemistry of sulfenic acids. 7. Reason for the high reactivity of sulfenic acids. Stabilization by intramolecular hydrogen bonding and electro-negativity effects, *J. Org. Chem.* 51, 1033–1040.
50. Davis, F. A., Jenkins, R. H., Jr., Rizvi, S. Q. A., and Yocklovich, S. G. (1981) Chemistry of sulfenic acid. 3. studies of sterically hindered sulfenic acids using flash vacuum pyrolysis, *J. Org. Chem.* 46, 3467–3474.

51. Benitez, L. V., and Allison, W. S. (1974) The inactivation of the acyl phosphatase activity catalyzed by the sulfenic acid form of glyceraldehyde 3-phosphate dehydrogenase by dimedone and olefins, *J. Biol. Chem.* **249**, 6234–6243.
52. Reddy, S., Jones, A. D., Cross, C. E., Wong, P. S., and van der Vliet, A. (2000) Inactivation of creatine kinase by S-glutathionylation of the active-site cysteine residue, *Biochem. J.* **347**, 821–827.
53. Klatt, P., Pineda Molina, E., Lacoba, M. G., Padilla, C. A., Martinez Galisteo, E., Barcena, J. A., and Lamas, S. (1999) Redox regulation of c-Jun DNA binding by reversible S-glutathiolation, *FASEB J.* **13**, 1481–1490.
54. Cappiello, M., Voltarelli, M., Cecconi, I., Vilardo, P. G., Dal Monte, M., Marini, I., Del Corso, A., Wilson, D. K., Quirocho, F. A., Petrash, J. M., and Mura, U. (1996) Specifically targeted modification of human aldose reductase by physiological disulfides, *J. Biol. Chem.* **271**, 33539–33544.
55. Jabusch, J. R., Farb, D. L., Kerschensteiner, D. A., and Deutsch, H. F. (1980) Some sulfhydryl properties and primary structure of human erythrocyte superoxide dismutase, *Biochemistry* **19**, 2310–2316.
56. Kajihara, J., Enomoto, M., Seya, K., Sukenaga, Y., and Katoh, K. (1988) Physicochemical properties of charge isomers of recombinant human superoxide dismutase, *J. Biochem.* **104**, 638–642.
57. Liu, H., Zhu, H., Eggers, D. K., Nersissian, A. M., Faull, K. F., Goto, J. J., Ai, J., Sanders-Loehr, J., Gralla, E. B., and Valentine, J. S. (2000) Copper²⁺ binding to the surface residue cysteine 111 of His46Arg human copper–zinc superoxide dismutase, a familial amyotrophic lateral sclerosis mutant, *Biochemistry* **39**, 8125–8132.
58. Yamazaki, Y., Takao, T., Murata, H., Kawaharada, Y., Sugiyama, T., and Shimonishi, Y. (1997) The use of capillary liquid chromatography/electrospray mass spectrometry to identify a specific cysteine residue susceptible to S-thiolation in recombinant human Cu,Zn superoxide dismutase, *Res. Commun. Biochem. Cell Mol. Biol.* **1**, 205–217.
59. Deng, H. X., Hentati, A., Tainer, J. A., Iqbal, Z., Cayabyab, A., Hung, W. Y., Getzoff, E. D., Hu, P., Herzfeldt, B., Roos, R. P., et al. (1993) Amyotrophic lateral sclerosis and structural defects in Cu,Zn superoxide dismutase, *Science* **261**, 1047–1051.
60. Ishii, T., Sunami, O., Nakajima, H., Nishio, H., Takeuchi, T., and Hata, F. (1999) Critical role of sulfenic acid formation of thiols in the inactivation of glyceraldehyde-3-phosphate dehydrogenase by nitric oxide, *Biochem. Pharmacol.* **58**, 133–143.
61. MacQuarrie, R. A., and Bernhard, S. A. (1971) Mechanism of alkylation of rabbit muscle glyceraldehyde 3-phosphate dehydrogenase, *Biochemistry* **10**, 2456–2466.
62. Parker, D. J., and Allison, W. S. (1969) The mechanism of inactivation of glyceraldehyde 3-phosphate dehydrogenase by tetrathionate, *o*-iodosobenzoate, and iodine monochloride, *J. Biol. Chem.* **244**, 180–189.
63. Birkett, D. J. (1973) Mechanism of inactivation of rabbit muscle glyceraldehyde 3-phosphate dehydrogenase by ethacrynic acid, *Mol. Pharmacol.* **9**, 209–218.
64. Marley, R., Patel, R. P., Orie, N., Ceaser, E., Darley-Usmar, V., and Moore, K. (2001) Formation of nanomolar concentrations of S-nitroso-albumin in human plasma by nitric oxide, *Free Radical Biol. Med.* **31**, 688–696.
65. Tanner, J. J., Hecht, R. M., and Krause, K. L. (1996) Determinants of enzyme thermostability observed in the molecular structure of *Thermus aquaticus* D-glyceraldehyde-3-phosphate dehydrogenase at 25 Å resolution, *Biochemistry* **35**, 2597–2609.
66. Didierjean, C., Rahuel-Clermont, S., Vitoux, B., Dideberg, O., Branlant, G., and Aubry, A. (1997) A crystallographic comparison between mutated glyceraldehyde-3-phosphate dehydrogenases from *Bacillus stearothermophilus* complexed with either NAD⁺ or NADP⁺, *J. Mol. Biol.* **268**, 739–759.
67. He, X. M., and Carter, D. C. (1992) Atomic structure and chemistry of human serum albumin, *Nature* **358**, 209–215.
68. Finley, J. W., Wheeler, E. L., and Witt, S. C. (1981) Oxidation of glutathione by hydrogen peroxide and other oxidizing agents, *J. Agric. Food Chem.* **29**, 404–407.

BI0359240